REPORT DOCUMENTATION PAGE

Form Approved
OMB NO. 0704-0188

Public Reporting burden for this collection of information is estimated to average 1 hour per response, including the time for reviewing instructions, searching existing data sources, gathering and maintaining the data needed, and completing and reviewing the collection of information. Send comment regarding this burden estimates or any other aspect of this collection of information, including suggestions for reducing this burden, to Washington Headquarters Services, Directorate for information Operations and Reports, 1215 Jefferson Davis Highway, Suite 1204, Arlington, VA 22202-4302, and to the Office of Management and Budget, Paperwork Reduction Project (0704-0188,) Washington, DC 20503.

1. AGENCY USE ONLY (Leave Blank)	2. REPORT DATE	3. REPORT TYPE AND DATES COVERED Reprint
4. TITLE AND SUBTITLE See Attached Report		5. FUNDING NUMBERS DAAD19-00-1-0490
6. AUTHOR(S) See Attached Report		
7. PERFORMING ORGANIZATION NAME(S) AND ADDRESS(ES) George Mason University 4400 University Dr. MSN 4C6 Fairfax, VA 22030-4444		8. PERFORMING ORGANIZATION REPORT NUMBER
9. SPONSORING / MONITORING AGENCY NAME(S) AND ADDRESS(ES) U. S. Army Research Office P.O. Box 12211 Research Triangle Park, NC 27709-2211		10. SPONSORING / MONITORING AGENCY REPORT NUMBER 41080.3-MS

11. SUPPLEMENTARY NOTES
The views, opinions and/or findings contained in this report are those of the author(s) and should not be construed as an official Department of the Army position, policy or decision, unless so designated by other documentation.

12 a. DISTRIBUTION / AVAILABILITY STATEMENT	12 b. DISTRIBUTION CODE
Approved for public release; availability unlimited	

13. ABSTRACT (Maximum 200 words)

See Attached Report

14. SUBJECT TERMS	15. NUMBER OF PAGES 7
	16. PRICE CODE

17. SECURITY CLASSIFICATION OR REPORT	18. SECURITY CLASSIFICATION ON THIS PAGE	19. SECURITY CLASSIFICATION OF ABSTRACT	20. LIMITATION OF ABSTRACT
UNCLASSIFIED	**UNCLASSIFIED**	**UNCLASSIFIED**	UL

NSN 7540-01-280-5500

Standard Form 298 (Rev.2-89)
Prescribed by ANSI Std. 239-18
298-102

20040713 018

HTML ABSTRACT + LINKS

JOURNAL OF APPLIED PHYSICS VOLUME 95, NUMBER 1 1 JANUARY 2004

Deep-level transient spectroscopy study on double implanted n^+-p and p^+-n 4H-SiC diodes

Souvick Mitra and Mulpuri V. Rao[a)]
Department of Electrical and Computer Engineering, George Mason University, Fairfax, Virginia 22030-4444

N. Papanicolaou
Naval Research Laboratory, Washington, D.C. 20375

K. A. Jones and M. Derenge
Army Research Laboratory, Adelphi, Maryland 20783-1197

O. W. Holland
Department of Physics, University of North Texas, Denton, Texas 76203-4127

R. D. Vispute
Department of Physics, University of Maryland, College Park, Maryland 20742

S. R. Wilson
Digital DNA Labs, SPS, Motorola, Tempe, Arizona 85284

(Received 17 February 2003; accepted 15 September 2003)

Planar n^+-p and p^+-n junction diodes, fabricated in 4H-SiC epitaxial layers using a double-implantation technology (a deep-range acceptor followed by a shallow-range donor implantation and vice versa), are characterized using capacitance deep-level transient spectroscopy (DLTS) to detect deep levels, which may influence device electrical performance. Either Al or B was used as the acceptor, while N or P was used as the donor, with all implants performed at 700 °C and annealed at 1600–1650 °C with an AlN protection cap. Different traps were observed for the various dopants, which are believed to be related to different impurity-defect complexes. A trap at $\sim E_V + 0.51$ eV was observed in nitrogen-implanted samples, while an acceptor trap at $\sim E_V + 0.28$ eV and a donor trap at $\sim E_C - 0.42$ eV were observed in Al-implanted samples. A prominent boron-related D-center trap at $\sim E_V + 0.63$ eV is seen in the DLTS spectra of B-implanted diodes. In diodes with implanted phosphorus, three traps at $\sim E_V + 0.6$ eV, $E_V + 0.7$ eV, and $E_V + 0.92$ eV, are seen, which are not observed for implantations of other species. © 2004 American Institute of Physics. [DOI: 10.1063/1.1623631]

I. INTRODUCTION

Silicon carbide (SiC) is an important material for fabricating high-power,[1–4] high-temperature,[5–7] and high-frequency[8,9] devices because it has high thermal conductivity, large saturation electron drift velocity, high electric breakdown field, and excellent thermal stability. Ion implantation doping of SiC is an attractive method for use in fabricating planar devices.[10,11] A double-implantation process, consisting of a deep-range acceptor/donor implant followed by a shallow-range donor/acceptor implant, is necessary for making complementary field-effect transistors and several high-power devices such as thyristors and IGBTs. For the junctions to withstand high-blocking voltages in high-power devices, the lightly doped side of the junction needs to be deep, requiring high-energy ion implantation. It is, therefore, very interesting and important to study and characterize the deep-level defects created by the implantation/annealing doping process, which might limit the device performance. Deep-level transient spectroscopy (DLTS) is an excellent way to evaluate these defects.

Despite the importance of the n^+-p and p^+-n junctions created by the double-implantation process and their application to power switching devices, there have been no reports on DLTS characterization of double-implanted diodes on 4H-SiC to our knowledge. Other groups have studied single-implant vertical diode structures, either by n-type ion implantation into p-type epilayers[12] or by p-type ion implantation into n-type epilayers.[13,14] In this work, planar n^+-p and p^+-n junction diodes were made using successive selective-area, multiple-energy acceptor (Al or B) and donor (N or P) implants, and were subsequently characterized to determine the implantation-doping-process-induced deep levels. Implantation-related traps and intrinsic defect traps present in the depletion layer were studied in detail using capacitance DLTS for these two devices. All of these traps were characterized by their activation energies, cross-sectional areas, and possible origins.

II. EXPERIMENT

A. Device fabrication

Planar, circular p^+-n or n^+-p junction diodes were fabricated in p- or n-type ($4\times10^{15}\,\mathrm{cm}^{-3}$) 4H-SiC epilayers

a)Electronic mail: rmulpuri@gmu.edu

 © 2004 American Institute of Physics

Downloaded 03 Apr 2004 to 129.174.45.115. Redistribution subject to AIP license or copyright, see http://jap.aip.org/jap/copyright.jsp

TABLE I. Implant schedule used for making junction diodes by double implantations.

	Deep implant schedule		Shallow implant schedule	
Device	Energy/dose	Conc./ depth	Energy/dose	Conc./ depth
n^+-p diode	Al schedule 1 MeV/2.0×10^{12} cm^{-2} 600 keV/2.5×10^{12} cm^{-2} 360 keV/2.0×10^{12} cm^{-2} 200 keV/1.4×10^{12} cm^{-2} 90 keV/8.0×10^{11} cm^{-2} or B schedule 700 keV/2.2×10^{12} cm^{-2} 450 keV/2.0×10^{12} cm^{-2} 260 keV/1.8×10^{12} cm^{-2} 150 keV/1.4×10^{12} cm^{-2} 80 keV/1.0×10^{12} cm^{-2} 40 keV/6.0×10^{11} cm^{-2}	1×10^{17} cm^{-3}/ 1 μm	N schedule 145 keV/2.2×10^{14} cm^{-2} 90 keV/1.4×10^{14} cm^{-2}	2×10^{19} cm^{-3}/ 0.2 μm
p^+-n diode	N schedule 1.2 MeV/2.42×10^{12} cm^{-2} 800 keV/2.2×10^{12} cm^{-2} 500 keV/1.9×10^{12} cm^{-2} 300 keV/1.6×10^{12} cm^{-2} 170 keV/1.35×10^{12} cm^{-2} 90 keV/8.88×10^{11} cm^{-2} 30 keV/1.8×10^{11} cm^{-2} or P schedule 1.4 MeV/3.06×10^{12} cm^{-2} 900 keV/2.23×10^{12} cm^{-2} 650 keV/1.60×10^{12} cm^{-2} 450 keV/1.35×10^{12} cm^{-2} 300 keV/1.37×10^{12} cm^{-2} 170 keV/8.99×10^{11} cm^{-2} 90 keV/4.49×10^{11} cm^{-2}	1×10^{17} cm^{-3}/ 1 μm	Al schedule 160 keV/1.37×10^{15} cm^{-2} 80 keV/6.72×10^{14} cm^{-2} 40 keV/3.23×10^{14} cm^{-2} 20 keV/1.54×10^{14} cm^{-2}	1×10^{20} cm^{-3}/ 0.2 μm

grown on the Si-face, 8° off-axis, p^+- or n^+-4H-SiC substrates, respectively. Deep n- or p-type regions were created by selective-area, multiple-energy, box profile nitrogen (or phosphorus) or boron (or aluminum) ion implantations, respectively. Shallow p^+ or n^+ regions were formed similarly by selective-area, multiple-energy, box profile implants of Al or N, respectively. The implant schedules and the resulting volumetric doping densities are given in Table I. To obtain reliable ohmic contacts, a shallow implant (at a single energy) yielding $2\times10^{19}\,\mathrm{cm}^{-3}$ N or $1\times10^{20}\,\mathrm{cm}^{-3}$ Al was performed for both n- and p-type regions, respectively, in the area where the planar ohmic metal contacts were placed. All implants were performed at 700 °C using a thick (2.5 μm) SiO_2 layer as an implant mask layer. The diodes were annealed at 1600–1650 °C for 10 min using an AlN encapsulant. Ohmic contacts were formed by e-beam evaporation of Ni and Ti/Al on n- and p-type regions, respectively, and alloyed at 1200 °C for 3 min in a vacuum system. No junction termination was used. The diameter of the diode junction is 245 μm. The p^+-n junction device structure is shown in Fig. 1. The n^+-p device structure is similar to that of Fig. 1 with n layers in place of p layers and vice versa. We used SiO_2 passivation for the diodes.

B. DLTS setup

The detection of deep levels in SiC double-implanted diodes was performed using a computer controlled fully automated DLTS system from BIORAD. The accuracy of the

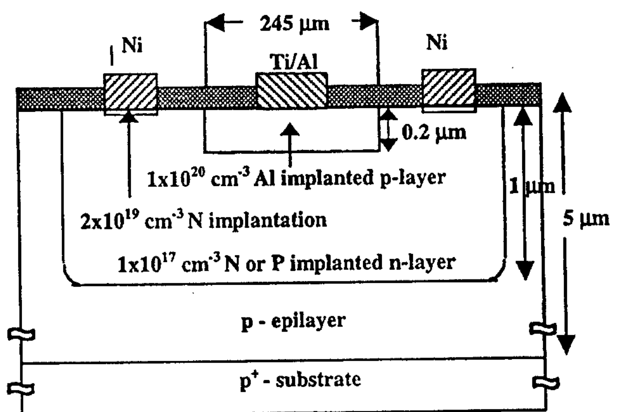

FIG. 1. Cross-sectional view of p^+-n junction diode.

Downloaded 03 Apr 2004 to 129.174.45.115. Redistribution subject to AIP license or copyright, see http://jap.aip.org/jap/copyright.jsp

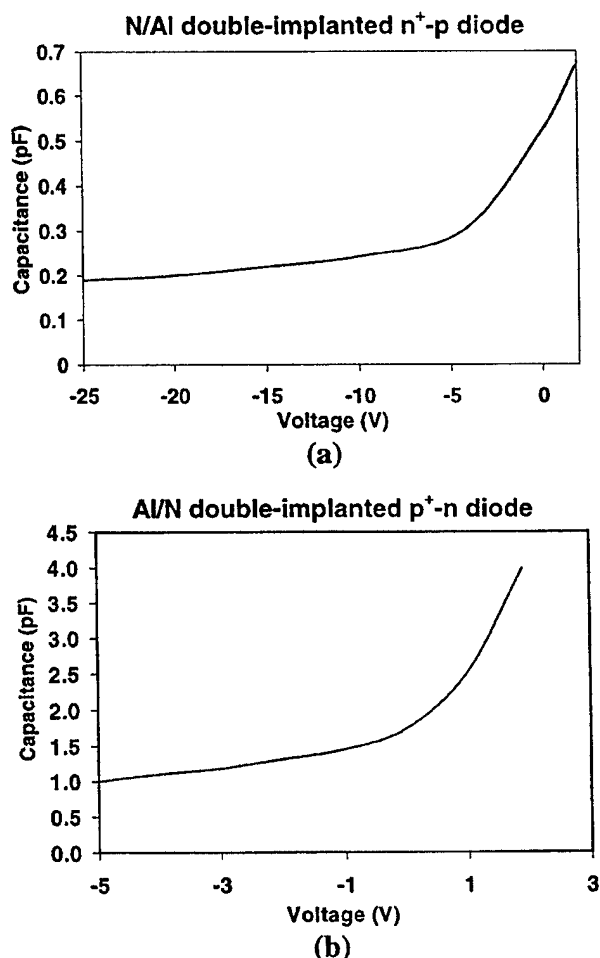

FIG. 2. Typical $C-V$ curves for (a) n^+-p and (b) p^+-n diodes.

measurement was improved by compensating and calibrating sample capacitance, optimizing physical/experimental parameters, and averaging a large number of temperature transients. Capacitance DLTS was performed for n^+-p and p^+-n double-implanted diodes using filling pulses of variable height and duration at different reverse-bias voltages needed to sweep the junction interface into depletion. The DLTS system used in this study works well in the temperature range of 100 to 600 K. We performed our measurements in the temperature range from 200 to 550 K. It should be noted that since thermal scans were performed below 600 K due to the system limitations, the observation of deep levels is restricted to about 1 eV from the band edges. We did not perform measurements below 200 K, because no significant DLTS peaks were observed for the emission window we used for the measurement. Typical $C-V$ curves are shown in Figs. 2(a) and 2(b), respectively, for n^+-p and p^+-n diodes. This $C-V$ data is used for calculating the trap density.

III. RESULTS AND DISCUSSION

A. Basic electrical characteristics

A room-temperature leakage current of 5×10^{-8} A/cm^2 was observed at a 20 V reverse bias for the N/B dual-implanted n^+-p diode, which increased to 3.3×10^{-7} A/cm^2 at 250 °C. The N/Al dual-implanted n^+-p diode had a room-temperature leakage current of 6.4×10^{-7} A/cm^2 at 20 V reverse bias, which increased to 1.7×10^{-4} A/cm^2 at 250 °C. A higher leakage current in Al-implanted diodes is probably due to a higher residual implant damage compared to the B-implanted diodes. Detailed $I-V-T$ characteristics of n^+-p junction diodes are reported elsewhere.[15] A significantly low leakage current up to a 20 V reverse bias offered suitable conditions for performing capacitance DLTS measurements on n^+-p diodes in this study. A higher leakage current ($\sim8\times10^{-2}$ A/cm^2 at a reverse bias of 4 V for Al/N double-implanted diodes) is observed compared to the n^+-p diodes, for the same reverse voltage for both Al/N and Al/P dual-implanted p^+-n diodes. This might be due to a higher degree of damage created by the Al implantation, used for the p^+-layer formation in the p^+-n diodes compared to the nitrogen implantation used for the n^+-layer formation in the n^+-p diodes. As shown in Table I, the implant doses used for the p^+ region of p^+-n diodes are higher than those for the n^+ region of n^+-p diodes. This is done to compensate for the high carrier activation energy for the p-type dopants ($E_A\geq200$ meV) in 4H-SiC compared to donors ($E_D\sim70$ meV). In addition, a higher atomic mass of Al (used for p^+-layer formation) compared to N (used for n^+-layer formation) results in a greater implant damage for the p^+-n diodes compared to the n^+-p diodes. The n^+-p and p^+-n diodes are processed in two different runs. Surface leakage may also contribute to the high leakage currents.

B. DLTS measurements

Using the DLTS spectrum, the Arrhenius plots, and the $C-V$ characteristics, we have determined the thermal activation energy (E_a), capture cross-section (σ), and trap density/concentration (N_t) for each defect level that appeared as a peak in the DLTS spectrum using the familiar Lang's method.[16]

1. n^+-p diodes

For the n^+-p diodes, a reverse-bias voltage of 20 V was applied during the DLTS measurements. The doping concentration of the nitrogen-implanted region ($\sim2\times10^{19}$ cm^{-3}) is more than two orders of magnitude higher than the doping concentration of the p-type region (1×10^{17} cm^{-3}); hence, the depletion region of the junction diode expands mostly into the acceptor region, with a very shallow spread over the donor side. To obtain an optimal DLTS spectrum having the best possible trap signature, the emission rate window was varied between 20.48 ms and 2.03 s. A typical DLTS spectrum and corresponding Arrhenius plot for the N/Al dual-implanted diodes, obtained at a reverse bias of 20 V, a forward filling pulse of 1 V, and a rate window of 20.48 ms are shown in Figs. 3(a) and 3(b), respectively. The typical DLTS spectrum reveals a hump in the low-temperature range (220–280 K), which could be formed by two poorly resolved deep centers. Measurements done with a different rate window (2.03 s) and pulse voltage (2 V) indicated the presence of one acceptor (0.28 eV, N1Al) and one donor level (0.42 eV,

Downloaded 03 Apr 2004 to 129.174.45.115. Redistribution subject to AIP license or copyright, see http://jap.aip.org/jap/copyright.jsp

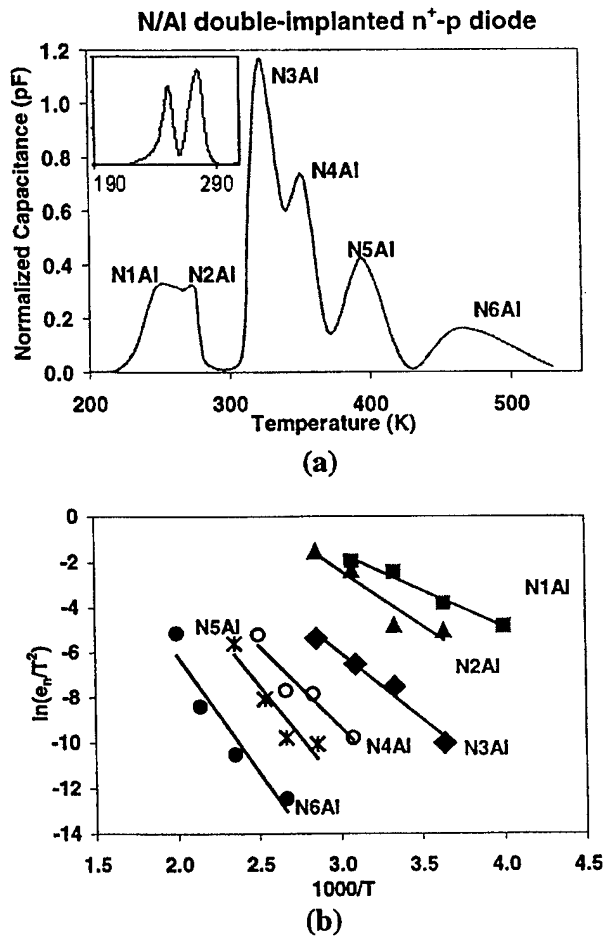

FIG. 3. (a) Typical DLTS spectrum and (b) corresponding Arrhenius plot, for N/Al double-implanted n^+–p diodes.

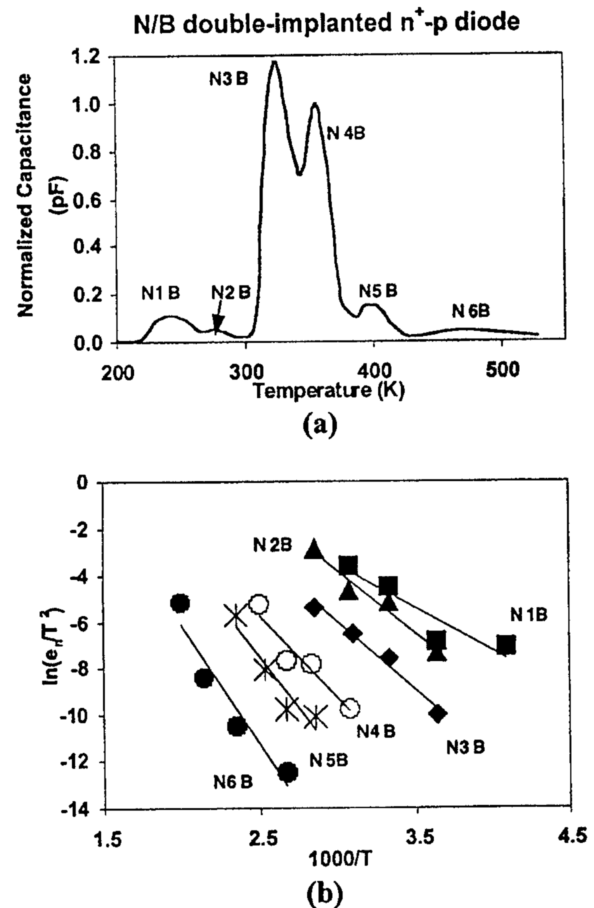

FIG. 4. (a) Typical DLTS spectrum and (b) corresponding Arrhenius plot, for N/B double-implanted n^+–p diodes.

N2Al) distinct peaks, as shown in the inset of Fig. 3(a). These peaks are believed to be introduced by the Al implants. Fung *et al.*[14] and Troffer *et al.*[17] reported similar deep centers in Al-implanted SiC.

The trap located at E_V+0.51 eV (N3Al) with a capture cross section of $6.5\times10^{-15}\,\mathrm{cm}^2$, is believed to be due to a complex involving nitrogen and ion-induced defects.[12] We have observed a peak with the same activation energy and cross section as that of N3Al in fully N-implanted metal–semiconductor field-effect transistors made in bulk semi-insulating 4H-SiC.[18,19] Nitrogen involved in the N3Al center is the nitrogen dopant in the n-type epitaxial layer (in which the n^+–p diode is formed) and nitrogen in the tail of the n^+ layer. The trap N4Al located at E_V+0.62 eV could be attributed to the D center,[12,20–22] which exhibits a deep acceptor behavior. The origins of the other two deep traps (N5Al and N6Al) at higher energies are discussed later.

A typical DLTS spectrum and corresponding Arrhenius plot obtained at a reverse bias of 20 V, a forward filling pulse of 1 V, and a rate window of 20.48 ms for the n^+–p diodes with a deep boron-implanted p-region and nitrogen-implanted shallow n^+ region, are presented in Figs. 4(a) and 4(b), respectively. Two dominant trap signatures, N3B and N4B, are observed, of which N3B has a similar activation energy and cross section as that of N3Al, which is attributed to a dopant-defect complex center involving the nitrogen. As shown in Fig. 5, the intensity of the trap N3Al/N3B decreases, with an increase of reverse-bias voltage. In other words, the trap concentration increases as the n^+/p metallurgical junction is approached, indicating that this region has a

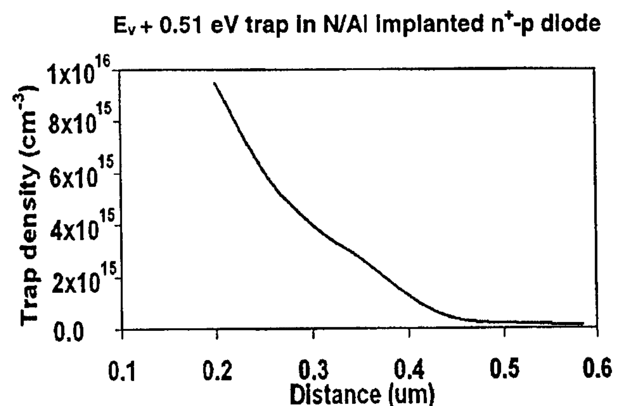

FIG. 5. Defect-concentration–junction-depth profile for N3Al peak in N/Al double-implanted n^+–p diodes. Highest trap concentration is observed near the physical junction.

Downloaded 03 Apr 2004 to 129.174.45.115. Redistribution subject to AIP license or copyright, see http://jap.aip.org/jap/copyright.jsp

higher defect concentration than the regions far away from the junction. This suggests that the origin of the N3Al/N3B trap involves ion-induced defects.

Another reason for the lower N3Al/N3B trap density at higher reverse voltages is the expansion of the depletion region into the p region, where the N dopant concentration is only the background N concentration of the n-type epitaxial layer used for the n^+-p junction formation, whereas at the lower reverse-bias voltages, a relatively high nitrogen concentration of the nitrogen implant tail of the n^+ region contributes to a higher nitrogen-defect complex concentration. In fact, the shape of Fig. 5 is similar to that of the implant tail. In the spectrum shown in Fig. 4(a), the N4B trap [which has the same activation energy as N4Al in Fig. 3(a)] looks more prominent than the N4Al trap, with a higher concentration ($\sim 10^{15}\,\text{cm}^{-3}$). This clearly indicates that this is due to the presence of D centers introduced by the boron implant, as reported by Gong *et al.*[13] Considering the activation energy (0.63 eV) and capture cross-section ($\sim 5\times 10^{-14}\,\text{cm}^2$), we found that the D center in this study matches well with the reported[20–22] values of known D center in SiC. The D center has been observed earlier[20–22] in B-implanted SiC, and is attributed to a complex formed by one B atom at a C site and a nearest-neighbor intrinsic divacancy defect. The B available in N/Al-implanted diodes is the unintentional background B (concentration $\sim 10^{15}\,\text{cm}^{-3}$) in the n-type epitaxial layer, whereas a large concentration ($\sim 10^{17}\,\text{cm}^{-3}$) of B is available in N/B-implanted diodes, resulting in a higher intensity N4B peak compared to the N4Al peak. The rest of the DLTS spectrum consists of two poorly resolved peaks at $\sim E_V+0.76\,\text{eV}$ (N5B) and $\sim E_V+0.88\,\text{eV}$ (N6B). The origins of these two peaks are unknown, but they are also seen in the DLTS spectra of Al implanted n^+-p diodes, shown in Fig. 3(a), as peaks N5Al and N6Al with a higher intensity than the N5B and N6B peaks in the B-implanted n^+-p diode. It is reasonable to conjecture that these two peaks are also Al-defect-complex-related deep levels.

2. p^+-n diodes

For the p^+-n diodes, a reverse-bias voltage of ~ -4 V was applied for DLTS measurements. A relatively low reverse bias was applied for the p^+-n diodes compared to the n^+-p diodes to avoid high leakage currents. To obtain an optimal DLTS spectrum having the best possible trap signature, the emission rate window was varied between 240.8 ms and 2.03 s. A typical DLTS spectrum and corresponding Arrhenius plot, for diodes made with a deep nitrogen-implanted n-type region and a shallow Al-implanted p^+-region, for a forward filling pulse of 2 V and a rate window of 20.48 ms are shown in Figs. 6(a) and 6(b), respectively. In this case, the trap centers, Al2N and Al3N, located at $E_t-E_V=0.27\,\text{eV}$ (acceptor trap) and $E_C-E_t=0.43\,\text{eV}$ (donor trap), respectively, are more prominent and sharper than the respective peaks, N1Al and N2Al, in the DLTS spectrum of N/Al-implanted n^+-p diodes shown in Fig. 3(a). The trap concentrations are also relatively higher (three orders of magnitude) compared to the n^+-p diodes, justifying the assignment of these peaks to the Al-related defect

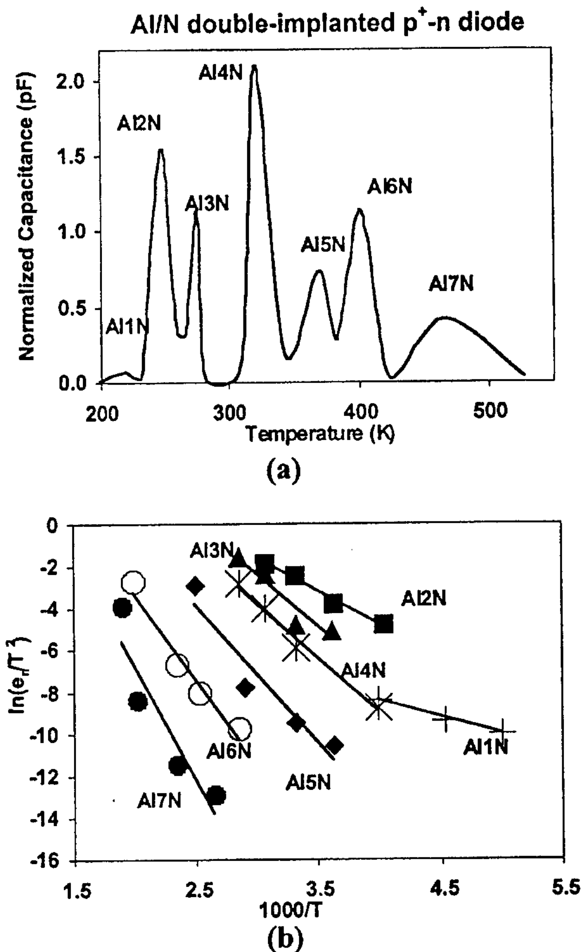

FIG. 6. (a) Typical DLTS spectrum and (b) corresponding Arrhenius plot, for Al/N double-implanted p^+-n diodes.

centers, made earlier. It is clear from Table I that the Al concentration in the p^+ region of the p^+-n diode is three orders higher than the Al concentration in the p region of the n^+-p diode. A defect center observed at $E_C-0.15\,\text{eV}$ (Al1N) for a rate window of 240.8 ms and a filling pulse of 3 V in the p^+-n diodes, could be attributed to a dopant-defect complex center formed due to a N dopant residing at the C lattice site.[23] The dominant trap, named as Al4N, located at $E_V+0.52\,\text{eV}$, and having a concentration, an order of magnitude higher than that of n^+-p diodes, could be attributed to a dopant-defect complex center involving a nitrogen dopant. A high defect concentration in Al-implanted p^+-n diodes and a high N concentration in the depletion region, which extends into the nitrogen implanted n region, may be responsible for a high concentration of this trap in the Al/N-implanted p^+-n diodes. This trap did not appear as a distinct peak in the spectrum of Al/P double-implanted p^+-n diodes because of the lack of nitrogen impurity in the diode, as discussed later. Two more acceptor traps labeled Al5N and Al6N, are also evident in the typical DLTS spectrum of an Al/N double-implanted p^+-n diode with a capture cross section $\sim 10^{-16}\,\text{cm}^2$. Al5N ($E_V+0.62\,\text{eV}$) trap, as discussed earlier, is related to a D center involving boron background impurity. The defect center (Al6N) at E_V

Downloaded 03 Apr 2004 to 129.174.45.115. Redistribution subject to AIP license or copyright, see http://jap.aip.org/jap/copyright.jsp

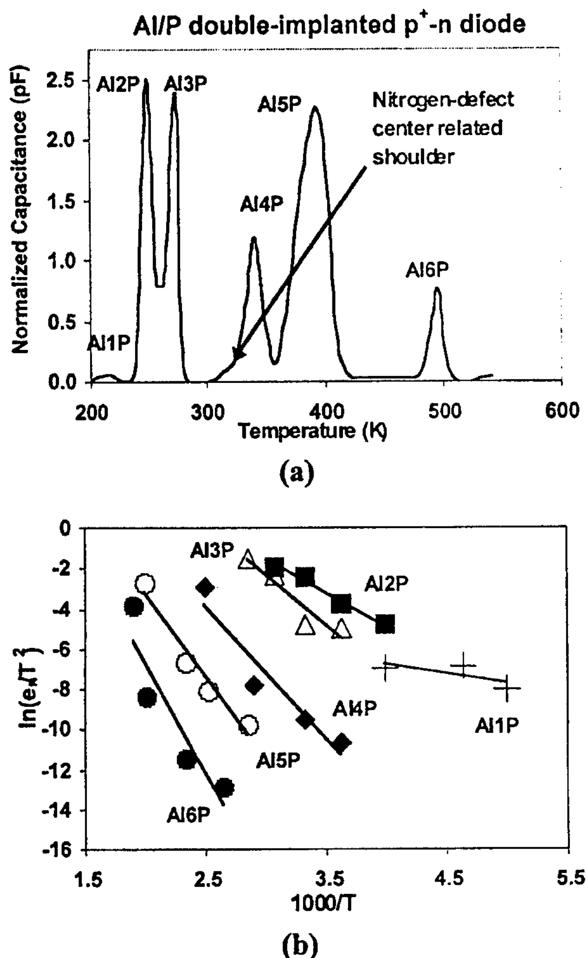

FIG. 7. (a) Typical DLTS spectrum and (b) corresponding Arrhenius plot, for Al/P double-implanted p^+-n diodes.

$+0.78$ eV can be attributed to a vacancy-related intrinsic defect configuration.[24] Its concentration is higher for the p^+-n diodes compared to the corresponding peaks in n^+-p diodes, probably because of a higher residual implant damage concentration in the p^+-n diodes.

The DLTS spectrum and corresponding Arrhenius plots for the p^+-n diodes with phosphorus-implanted n and Al-implanted p^+ regions, for a forward filling pulse of 2 V and a rate window of 20.48 ms are shown in Figs. 7(a) and 7(b), respectively. Trap centers similar to Al2N and Al3N in Fig. 6(a) (with the same activation energy and cross section), which are assigned to Al-defect complex centers, are seen as peaks labeled Al2P and Al3P with concentration $>1\times10^{19}\,\mathrm{cm}^{-3}$. Three other traps, labeled Al4P, Al5P, and Al6P, are observed in the spectrum with cross sections $\sim10^{-15}-10^{-17}\,\mathrm{cm}^2$ and a concentration $\sim10^{19}\,\mathrm{cm}^{-3}$. The nitrogen-defect center peak seen at $E_V+0.51$ eV [as N3Al in Fig. 3(a), N3B in Fig. 4(a), and Al4N in Fig. 6(a)] is not distinctly seen in Al/P-implanted p^+-n diodes. This is because no intentional nitrogen doping exists in this diode. It appears as a very low-intensity peak in the low-temperature shoulder of the Al4P peak. The only nitrogen present in the Al/P double-implanted diode is the very low-concentration ($<10^{14}\,\mathrm{cm}^{-3}$) unintentional background nitrogen in the p-type epitaxial layer used for making the p^+-n diode, whereas the other diodes contained nitrogen as a result of direct implantation or intentional doping of the n-type epitaxial layer. The Al4P peak at $E_V+0.6$ eV in Fig. 7(a) with a capture cross section of $\sim10^{-15}\,\mathrm{cm}^2$ and trap concentration of $\sim10^{18}\,\mathrm{cm}^{-3}$ is not seen in samples that do not have a phosphorus implant in them. A phosphorus-defect complex center may be responsible for this peak. The high-intensity Al5P peak and a sharp Al6P peak, seen in the Al/P-implanted diode, at $E_V+0.7$ eV and $E_V+0.92$ eV, respectively, [Fig. 7(a)], are also not seen in other diodes made in this study, which do not have a phosphorus implant in them. Phosphorus may be involved in the defect complex centers that are responsible for these peaks as well. A detailed study revealed that peak amplitude of the DLTS spectrum, corresponding to the peak Al5P ($E_V+0.7$ eV), achieved a constant value with the filling pulse time t_p and it clearly emphasizes the role of a point defect as the origin of this peak. It showed a consistently increasing trap concentration towards the junction interface. These traps that are present at high concentrations at the junction interface strongly influence the device $I-V$ characteristics. Most of these traps originate as a result of residual implant lattice damage or the implant-defect complexes.

IV. SUMMARY

Deep levels in the double-implanted n^+-p (N–Al/B) and p^+-n (Al–N/P) diodes made in 4H-SiC, were studied using the capacitance DLTS technique. The high leakage current behavior of the p^+-n junction diodes was analyzed using the DLTS data, which clearly revealed a higher magnitude of trap concentrations in these devices compared to the n^+-p diodes. A high degree of implant damage created by higher dose Al implantations (used for p^+ region) of the p^+-n diodes compared to a relatively lower dose and lighter N implantations (used for n^+ region) of the n^+-p diodes is believed to be responsible for a higher trap concentration and a higher reverse leakage current density in the p^+-n diodes. All of the nitrogen-implanted diodes showed a prominent peak at 0.5–0.52 eV above E_V, which is identified as a trap created by a nitrogen-defect complex center. Concentration of this trap has its highest value near the physical junction of the diodes, which clearly indicates the role of ion-induced damage in the formation of this trap.

For all Al-implanted n^+-p and p^+-n diodes, two prominent peaks at $\sim E_C-0.27$ eV and $\sim E_V+0.42$ eV, originating from Al-defect complex centers, were observed. For the n^+-p devices, where Al implantation was used to form the deep p region, these traps are distributed in the concentration range of $10^{15}\,\mathrm{cm}^{-3}$, whereas for the p^+-n junction diodes, where Al implantation is used for the shallow p^+-region formation, density of these traps increased to $\sim10^{19}\,\mathrm{cm}^{-3}$. In addition, a B-related D-center trap at $\sim E_V+0.63$ eV is seen in the DLTS spectrum of all diodes, except for the p^+-n devices made with a phosphorus-implanted deep n region.

Downloaded 03 Apr 2004 to 129.174.45.115. Redistribution subject to AIP license or copyright, see http://jap.aip.org/jap/copyright.jsp

TABLE II. Traps observed in double implanted junction diodes in this study.

Trap	Peak location (eV)	Cross section (cm^2)	Possible origin
N1Al, Al2N, Al2P	$E_V+0.27$	7.0×10^{-14}	Al implantation
N2Al, Al3N, Al3P	$E_C-0.43$	7.5×10^{-14}	Al implantation
N3Al, N3B, Al4N	$E_v+0.51$	6.5×10^{-15}	Nitrogen-defect complex
N4Al, N4B, Al5N	$E_v+0.62$	5.0×10^{-14}	D center
N5Al	$E_v+0.76$	$4-7\times10^{-14}$	Al-defect complex
N6Al, Al7N	$E_v+0.88$	$4-7\times10^{-14}$	Al-defect complex
N1B	$E_V+0.32$	$\sim10^{-14}$	Not known
N2B	$E_C-0.46$	$\sim10^{-14}$	Not known
Al1N	$E_C-0.15$	5×10^{-15}	Nitrogen at C-site defect complex
Al6N	$E_V+0.78$	6.0×10^{-17}	Vacancy-related intrinsic defect
Al1P	$E_V+0.08$	3.4×10^{-16}	Not known
Al4P	$E_V+0.6$	1.4×10^{-15}	Phosphorus-defect complex
Al5P	$E_V+0.7$	1.6×10^{-15}	Phosphorus-defect complex
A6P	$E_V+0.92$	9×10^{-15}	Not known

Three distinct peaks at $\sim E_V+0.6$ eV, $E_V+0.7$ eV, and $E_V+0.92$ eV are observed in phosphorus-implanted diodes. The deep center at $E_V+0.7$ eV can be attributed to a point defect. Various traps observed in this work and their possible origins are summarized in Table II. A higher deep-level defect concentration ($10^{18}-10^{19}\,cm^{-3}$) is found in the p^+-n devices compared to the n^+-p diodes. The origin of some of the traps and their influence on device performance are not clearly understood at this point. Higher trap concentrations in the p^+-n diodes compared to the n^+-p diodes led to a higher reverse leakage current in the p^+-n diodes.

ACKNOWLEDGMENT

This work is supported by ARO (Dr. Prater) under Grant No. DAAD19-00-1-0490.

[1] T. P. Chow and M. Ghezzo, Mater. Res. Soc. Symp. Proc. **423**, 9 (1996).
[2] J. A. Cooper, M. R. Melloch, J. M. Woodall, J. Spitz, K. J. Schoen, and J. P. Henning, Mater. Sci. Forum **264–268**, 895 (1998).
[3] D. M. Brown, E. Downey, M. Ghezzo, J. Kretchmer, V. Krishnamurthy, W. Hennessy, and G. Michon, Solid-State Electron. 39, 1541 (1996).
[4] S.-H. Ryu, A. K. Agarwal, R. Singh, and J. W. Palmour, IEEE Electron Device Lett. **22**, 127 (2001).
[5] T. Moore, EPRI J. **22**, 30 (1997).
[6] L. V. Rozario, L. P. Sadwick, R. J. Hwu, and D. B. King, *Proceedings of Fourth Intl. High Temperature Electronics Conference (HiTec)*, Albuquerque, NM, June, 1998, p. 29.
[7] W. Wondrak, R. Held, E. Niemann, and U. Schmid, IEEE Trans. Ind. Electron. **48**, 307 (2001).
[8] H. M. McGlothlin, D. T. Morisette, J. A. Cooper, Jr., and M. R. Melloch, *Conference Digest 57th Annual Device Research Conference*, 1999, p. 42.
[9] J. Eriksson, N. Rorsmann, and H. Zirath, Electron. Lett. **37**, 250 (2001).
[10] M. V. Rao, Solid-State Electron. **47**, 213 (2003).
[11] T. Kimoto, A. Itoh, N. Inoue, O. Takemura, T. Yamamoto, T. Nakajima, and H. Matsunami, Mater. Sci. Forum **264–268**, 675 (1998).
[12] K. Ghaffour, V. Lauer, A. Souifi, G. Guillot, C. Raynaud, S. Ortolland, M. L. Locatelli, and J. P. Chante, Mater. Sci. Eng., B **66**, 106 (1999).
[13] M. Gong, C. V. Reddy, C. D. Beling, S. Fung, G. Brauer, H. Wirth, and W. Skorupa, Appl. Phys. Lett. **72**, 2739 (1998).
[14] S. Fung, M. Gong, C. D. Beling, G. Brauer, H. Wirth, and W. Skorupa, J. Appl. Phys. **84**, 1152 (1998).
[15] J. B. Tucker, M. V. Rao, N. A. Papanicolaou, J. Mittereder, A. Elasser, A. W. Clock, M. Ghezzo, O. W. Holland, and K. A. Jones, IEEE Trans. Electron Devices **48**, 2665 (2001).
[16] D. V. Lang, J. Appl. Phys. **45**, 3023 (1974).
[17] T. Troffer, M. Schada, T. Frank, H. Itoh, G. Pensl, J. Heindl, H. P. Strunk, and M. Mayer, Phys. Status Solidi A **162**, 277 (1997).
[18] S. Mitra, M. V. Rao, K. Jones, N. Papanicolaou, and S. Wilson, Solid-State Electron. **47**, 193 (2003).
[19] S. Mitra, J. B. Tucker, M. V. Rao, N. Papanicolaou, and K. Jones, *Proc. ICSCRM '01, Intl. Conf. of Silicon Carbide and Related Materials 2001*, Material Science Forum, Vol. 389-393, 2002.
[20] W. Suttrop, G. Pensl, and P. Lanig, Appl. Phys. A: Solids Surf. **51**, 231 (1990).
[21] M. S. Mazzola, S. E. Saddow, P. G. Neudeck, V. K. Lakdawala, and S. We, Appl. Phys. Lett. **64**, 2730 (1994).
[22] S. E. Saddow, C. W. Tipton, M. S. Mazzola, P. G. Neudeck, and D. J. Larkin, Inst. Phys. Conf. Ser. **142**, 289 (1995).
[23] G. Pensl and W. J. Choyke, Physica B **185**, 264 (1993).
[24] A. V. Duijn-Arnold, T. Ikoma, O. G. Poluektov, P. G. Baranov, E. N. Mokhov, and J. Schmidt, Phys. Rev. B 57, 1607 (1998).

Downloaded 03 Apr 2004 to 129.174.45.115. Redistribution subject to AIP license or copyright, see http://jap.aip.org/jap/copyright.jsp